Electronic Supplementary Inofrmation

Lower ammoniation activation energy of CoN nanosheets by Mn doping with superior energy storage performance for secondary ion batteries

By *Lin Zhu, Ziliang Chen, Yun Song *, Pei Wang, Yingchang Jiang, Le Jiang, Yong-Ning Zhou, Linfeng Hu **

Department of Materials Science, Fudan University, Shanghai 200433 (P. R. China)

E-mail: songyun@fudan.edu.cn; linfenghu@fudan.edu.cn

Contents:

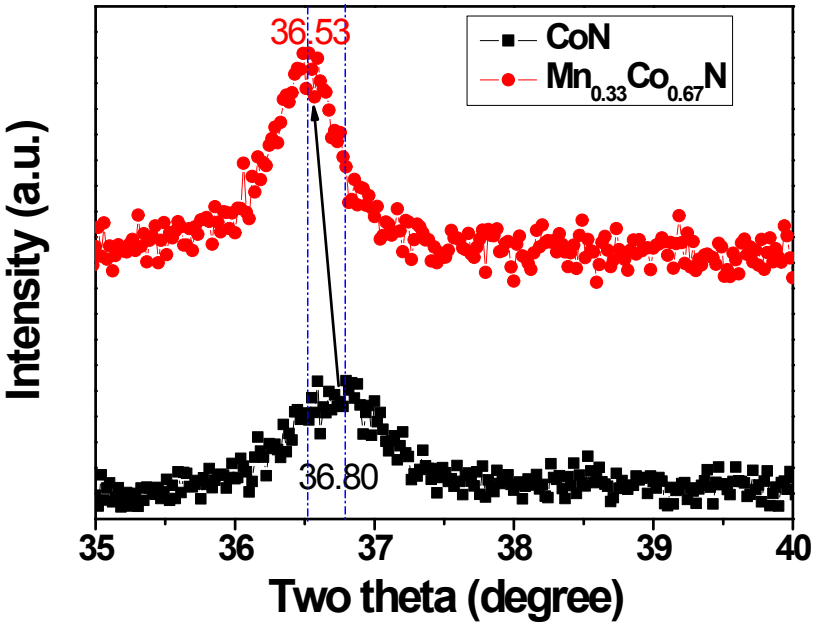

Figure S1. XRD comparison of $Mn_{0.33}Co_{0.67}N$ and CoN. Mn doping sample shift slightly to lower angle, causing by the radius of Mn^{2+}/Mn^{3+} (73 pm/67 pm) which is larger than Co^{3+} (61 pm).

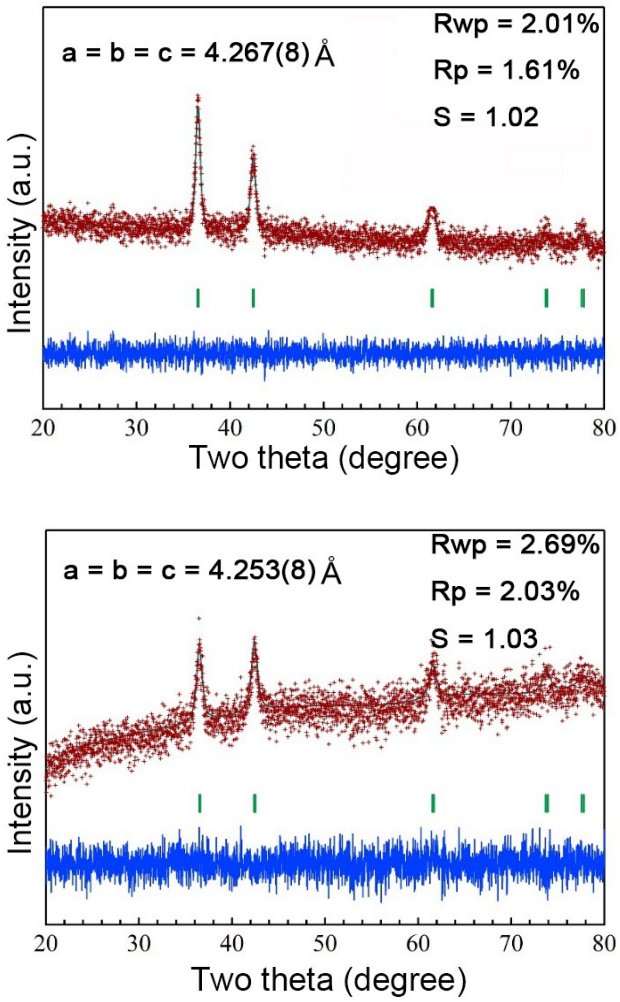

Figure S2. Rietveld refinement analysis of (a) $Mn_{0.33}Co_{0.67}N$ and (b) CoN, further confirming the slight angle shift.

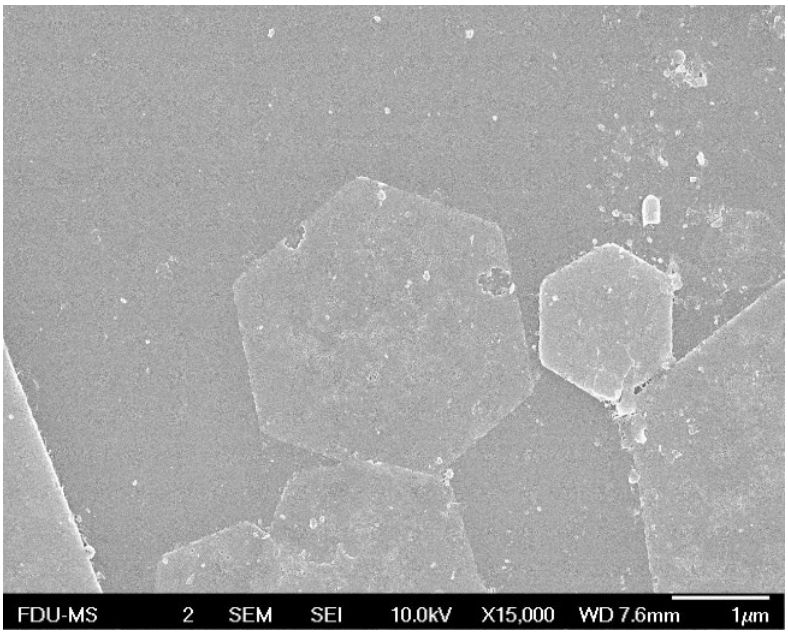

Figure S3. The SEM morphology of undoped CoN, showing the similar hexagonal nanosheets as the $Mn_{0.33}Co_{0.67}N$.

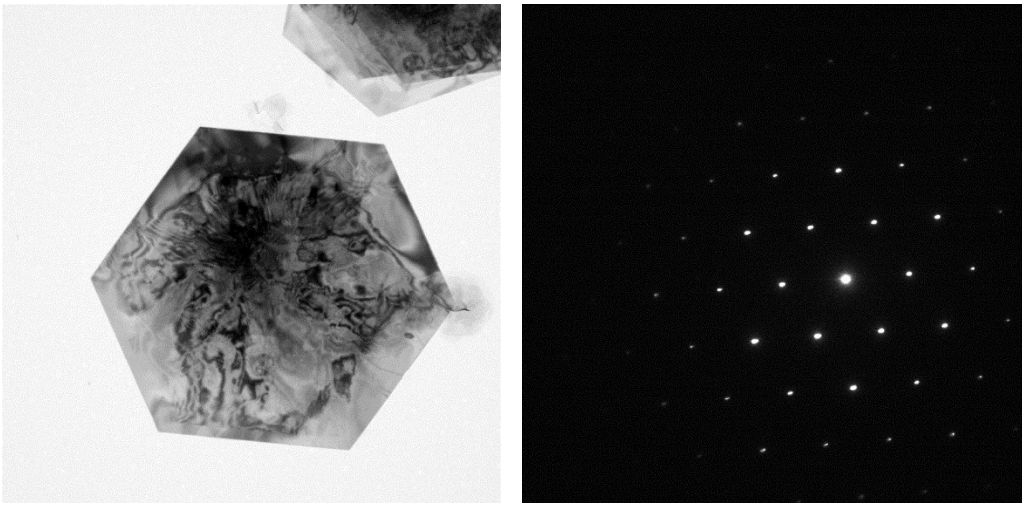

Figure S4. Typical TEM image and diffraction pattern of $Mn_{0.33}Co_{0.67}(OH)_{2.}$ The pristine $MnCo_2$-hydroxide shows well-developed 2D nanosheet morphology with a regular hexagonal frame, sharp corners and smooth surface.

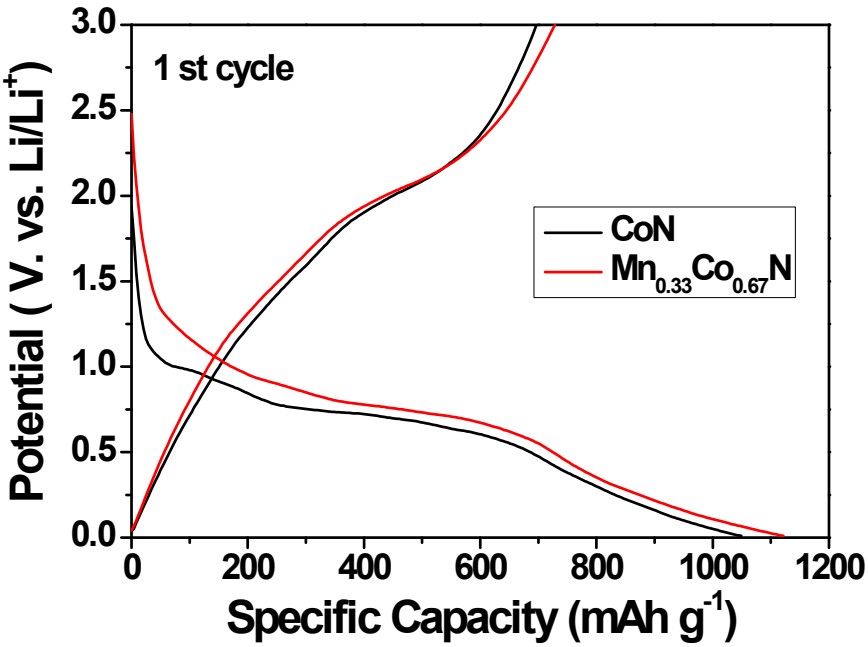

Figure S5. galvanostatic discharge-charge (GDC) voltage profiles of $Mn_{0.33}Co_{0.67}N$ and CoN for the 1st cycle.

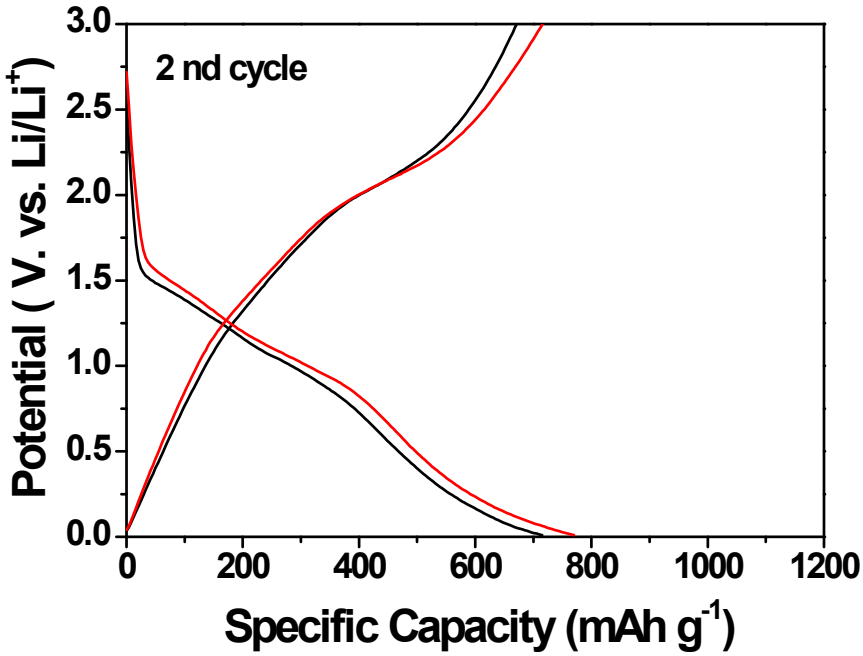

Figure S6. galvanostatic discharge-charge (GDC) voltage profiles of $Mn_{0.33}Co_{0.67}N$ and CoN for the 2nd cycle.

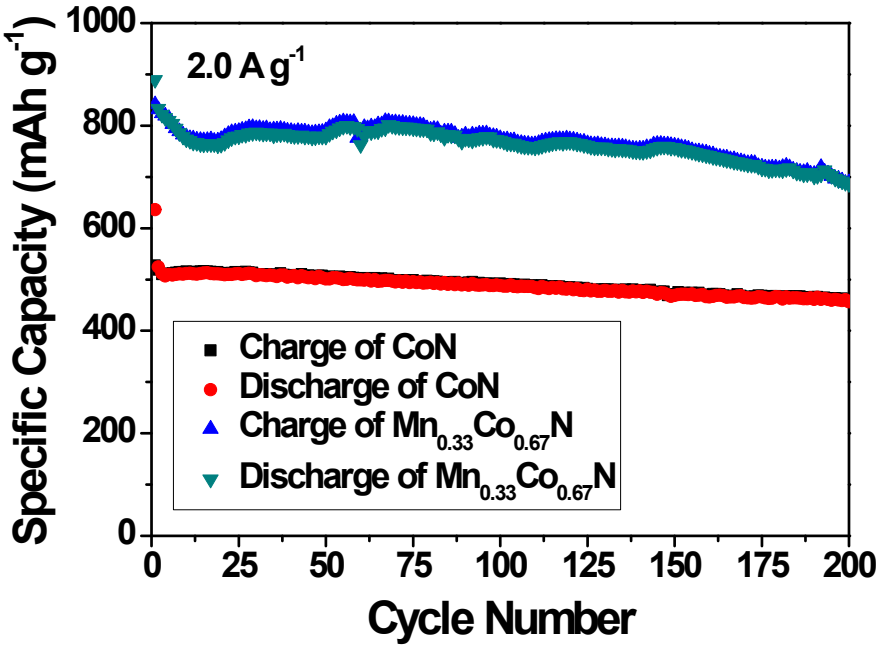

Figure S7. Comparative cycling performance of $Mn_{0.33}Co_{0.67}N$ and CoN at a current density of 2 A g^{-1}.

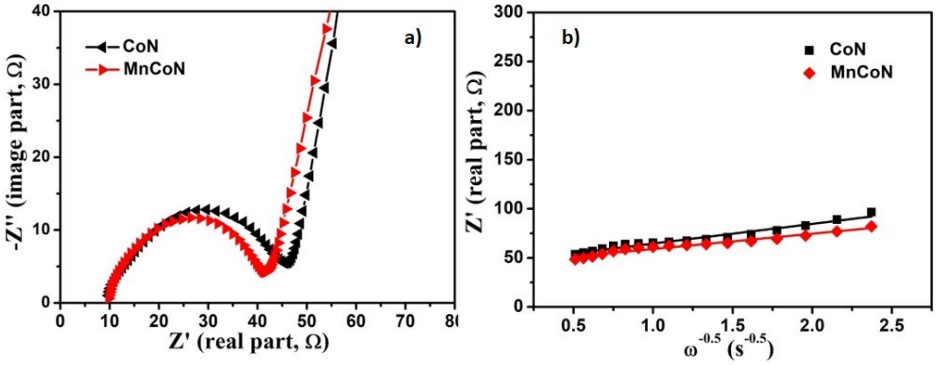

Figure S8. (a) Nyquist plots of $Mn_{0.33}Co_{0.67}N$ and CoN. (b) Relationship between Z_{Re} and $\omega^{-1/2}$ in the low frequency range. The EIS analysis has been added to further confirm the effect of Mn-doping. The Nyquist plots consist of depressed semi-circles and inclined lines. The semi-circle observed in the high and middle frequency range corresponds to the charge transfer resistance (R_{ct}) at the interface of the electrodes. After simulating the semi-circles of two samples using the equivalent circuit, values of R_{ct} of MnCoN and pure CoN are calculated to be 30.65 and 35.1 Ω, respectively. The smaller R_{ct} of MnCoN indicates that the electron transportation inside $Mn_{0.33}Co_{0.67}N$ is faster than that of pure CoN. The inclined lines in the lower frequency are attributed to the Warburg impedance, generally reflecting the lithium ion diffusion within the bulk electrode. The lithium ion diffusion coefficient can be calculated using the following equation:

$$D = 0.5\left(\frac{RT}{AF^2C\sigma_w}\right)^2$$

where D is the diffusion coefficient, R is the gas constant, T is the absolute temperature, F is Faraday's constant, A is the area of the electrode, C is the molar concentration of Li^+ ions, and σw is the Warburg factor, which can be calculated from the slope of the lines in Figure. S8b. The relation between Zre, square root of frequency ($\omega^{-1/2}$) and σ_w can be summarized as:

$$Z_{Re} = R_e + R_{ct} + \sigma_w \times \omega^{-1/2}$$

After linear fitting and calculating from equations above, the lithium diffusion coefficients of $Mn_{0.33}Co_{0.67}N$ and pure CoN are determined to be 1.46×10^{-14} and 2.82×10^{-15} $cm^2\ s^{-1}$, respectively. This result clearly suggests that Li ion diffusion is facilitated in $Mn_{0.33}Co_{0.67}N$ compared with pure CoN.